Electronic Supplementary Information

In-situ photodeposition of loaded Co-MoS_x for promoting visible-light g-C_3N_4 photocatalytic hydrogen production performance

Yonggang Lei[a,b,c], Kim Hoong Ng[d], Chenyu Zou[b], Lejun Chen[b], Yuekun Lai[b,c*], Jianying Huang[b,c*]

[a] College of Chemistry and Chemical Engineering, Hexi University, Zhangye 734000, PR China.

[b] National Engineering Research Center of Chemical Fertilizer Catalyst (NERC-CFC), College of Chemical Engineering, Fuzhou University, Fuzhou 350116, PR China

[c] Qingyuan Innovation Laboratory, Quanzhou 362801, PR China

[d] Department of Chemical Engineering, Ming Chi University of Technology, New Taipei City 243303, Taiwan

*Corresponding authors: jyhuang@fzu.edu.cn; yklai@fzu.edu.cn

1. Experimental section

1.1 Chemicals and materials

Urea (AR, 99%), Ammonium molybdate tetrahydrate (AR, 99%), Cobalt chloride hexahydrate (AR, 99%) all purchased from Sinopharm Group, and ammonium sulfide aqueous solution (20%) was purchased from Macklin. The deionized water used in the entire experiment was provided by Direct-Q 3UV from the French Mithberg company.

1.2 Characterization

The morphology of selected photocatalyst was revealed using scanning electron microscope (SEM; S-4800 instrument from Hitachi, Japan) while transmission electron microscope (TEM) images were recorded using the Zeiss Sigma instrument from Zeiss, Germany. X-ray diffractometer (XRD) patterns of photocatalyst were obtained using X'Pert3 made by Panalytical from Netherlands. Fourier transform infrared (FTIR) and X-ray photoelectron spectroscopy (XPS) spectra were examined by a Nicolet 6700 FTIR spectrometer and an Escalab-250Xi type X-ray photoelectron spectrometer from Thermo Fisher Scientific, USA, respectively. The UV-Vis absorption spectra was recorded using Lambda 950 UV-Vis NIR spectrophotometer from Perkin-Elmer, USA. Nitrogen physisorption isotherms were detected by an ASAP 2020M fully automated analyzer from Micrometric, USA, for specific surface area and pore size analysis. Luminescent photoluminescence (PL) spectra were tested using a Hitachi F-7000 fluorescence spectrophotometer from Japan at an excitation wavelength of 367 nm.

1.3 Preparation of catalysts

1.3.1 Preparation of CN

CN is prepared by pyrolysing 10 g urea in a corundum crucible at 500 ℃ for 2 h. A slow rate 5 ℃/min was employed to maximized the CN yield. The resulting faint yellow solid was grinded and stored in vial until further used or modification.

1.3.2 Preparation of MoS_x/CN

300 mg CN and required mass of $(NH_4)_2MoS_4$ was added to a reaction bottle filled with 100 mL of 10 vol.% ethanol solution. The suspension was stirred and purged by Ar, followed by 5 h-irradiation using xenon lamp ($\lambda > 400$ nm). The irradiation solid was filtered, dried and stored until used. Under the same preparation outline, MoS_x/CN photocatalysts with different MoS_x contents (MoS_2 wt.%=5, 10, 12, 15, and 20) were prepared by varying the mass of $(NH_4)_2MoS_4$. All prepared photocatalysts were labelled as MCN-X, where X is denoted for the mass percentage of MoS_x in the composite catalyst. Specifically, MCN-12 is abbreviated as MCN.

1.3.3 Preparation of Co-MoS_x/CN

A series of Co doped MoS_x/CN was prepared using the procedure described in preparation of MoS_x/CN with slight modification. Notable, the content of Co-MoS_x is fixed at 12 wt.% while the Co:MoS_x ratio was varied by using different amount of $CoCl_2 \cdot 6H_2O$ and $(NH_4)_2MoS_4$ (mass ratios of 1:3, 1:12, 1:21, 1:30, and 1:60) in the preparation. The obtained photocatalyst is labeled as Co-MCN (Y), where Y represents the mass ratio of Co to MoS_x. Specifically, Co-MCN (1:21) is abbreviated as Co-MCN. Co/CN, Fe-MCN, and Ni-MCN were prepared using the same method.

1.4 Photocatalytic H_2 evolution assessment

The photocatalytic hydrogen production experiment was carried out in a 100 mL sealed quartz reactor with a 300 W xenon lamp (Perfectlight, PLS-SXE300), which irradiated through a 400 nm cut-off filter. A condensate flow was maintained to control the temperature of setup throughout the reaction. Specifically, 10 mg of sample was added to 100 mL of triethanolamine solution (10 vol%) and bubbled with nitrogen for 10 minutes to eliminate O_2. Light was switched on to initiate the reaction and intermittent monitoring of hydrogen evolution was performed using gas chromatography (Shimadzu, GC-2014C). Following Eq 1 was used to determined the apparent quantum efficiency (AQE, %) of photocatalysts in the experiment irradiated with single-wavelength light source.

$$AQE\ (\%) = \frac{number\ of\ evolved\ H_2\ molecules \times 2}{number\ of\ incident\ photons} \times 100\% \quad (1)$$

1.5 Photo-electro-chemical (PEC) assessments of photocatalysts

The PEC performance of selected photocatalyst was evaluated using multifunctional electrochemical workstation (Solartron, Modulab XM) equipped with three-electrode system. Saturated Ag/AgCl electrode was employed as reference electrode while a 1 cm × 1 cm Pt foil was used as the counter electrode. The working electrode was prepared using conductive glass (FTO) over the drop coating method. In brief, 10 mg of well ground catalyst was dispersed in 250 μL DMF and 250 μL deionized water, followed by an addition of 40 μL Nafion (5 wt.%). After 30 min of ultrasonication, 60 μL of the slurry was dripped onto the FTO and dried naturally. By using Na_2SO_4 (0.5 M, pH=7) solution as electrolyte, the transient photocurrent density

was obtained in the presence of intermittent illumination with an interval of 30 seconds. During electrochemical impedance spectroscopy (EIS) testing, the bias voltage was fixed at open circuit potential while the frequency was set to 100 kHz to 0.1 Hz. Following Eq 2 was used for potential conversion from Ag/AgCl scale to RHE scale:

$$E_{RHE} = E_{Ag/AgCl} + 0.0591 \times pH + E^{\circ}_{Ag/AgCl} \quad (2)$$

Where $E_{Ag/AgCl}$ is denoted for the applied voltage and $E^{\circ}_{Ag/AgCl}$ stays constant at 0.1976 V under the room temperature of 25℃.

2. Synthesis of other cocatalysts.

Preparation of $(NH_4)_2MoS_4$: Under stirring conditions at room temperature, 1.5 g of $(NH_4)_6Mo_7O_{24}$ was added to 20 ml of $(NH_4)_2S$ solution, and heated at 80 ℃ for 2 h to obtain a dark red solution. After cooling to room temperature, transfer to a refrigerator and refrigerate for 24 h to obtain blood red crystals. Thoroughly wash the precipitated red blood crystals with anhydrous ethanol, dry and collect them, and store them under nitrogen.

Preparation of pristine MoS_x and Co-MoS_x: MoSx and Co-MoS_x were synthesized with reference to the literature[1], specifically by taking 1 mM MoS_x and ErB andADDINg them to a reaction vial containing 10 vol% triethanolamine solution, filtering the reaction precipitate after 5 h of light exposure, drying overnight under vacuum and grinding to obtain MoS_x. Co-MoS_x was synthesized with reference to MoS_x, the difference is the addition of $CoCl_2 \cdot 6H_2O$ and $(NH_4)_2MoS_4$ according to a mass ratio of 1:21.

Preparation of Fe-MoS_x/CN and Ni-MoS_x/CN catalysts: Fe-MoS_x/CN (Fe-MCN) and Ni-MoS_x/CN (Ni-MCN) were obtained by the same procedure of preparing Co-MoS_x/CN. The $CoCl_2$-$6H_2O$ added during the preparation of Co-MoS_x/CN was changed to $FeCl_3$ and $NiCl_2 \cdot 6H_2O$, respectively, to obtain Fe-MCN and Ni-MCN catalysts.

Preparation of Pt/CN catalyst: CN was added to a reaction flask containing 100 mL of triethanolamine solution (10 vol%), and then an appropriate amount of H_2PtCl_6 solution was added and mixed thoroughly by ultrasonication. The Pt/CN catalyst was obtained by evacuating and passing argon gas for protection and then photoluminescence for 1 h.

3. Calculation

The "12 wt%" is derived from stoichiometric calculations. We assume that all $(NH_4)_2MoS_4$ is generated as MoS_x under excess conditions and loaded on CN. The mass ratios were calculated as follows:

$$m_{MoS_x} = \frac{M_{MoS_x}}{M_{(NH_4)_2MoS_4}} \times m_{(NH_4)_2MoS_4}$$

$$Mass\ ratio = \frac{m_{MoS_x}}{m_{MoS_x} + m_{CN}} \times 100\%$$

Co-MoS_x, on the other hand, is calculated following the same procedure, only keeping the ratio of Co to MoS_x at 1:21.

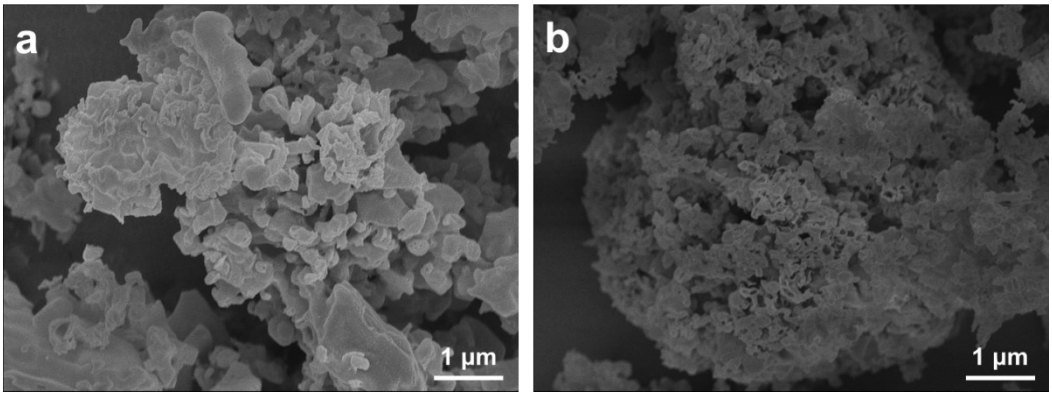

Fig. S1. The SEM image of (a) pure CN and (b) MCN

Table S1. BET specific surface area and pore volume of the samples.

Sample	BET specific surface area (m^2/g)	pore volume (cm^3/g)	Average pore size (nm)
CN	35.9	0.0501	5.5835
MCN	41.2	0.0615	5.9694
Co-MCN	30.8	0.0451	5.8569

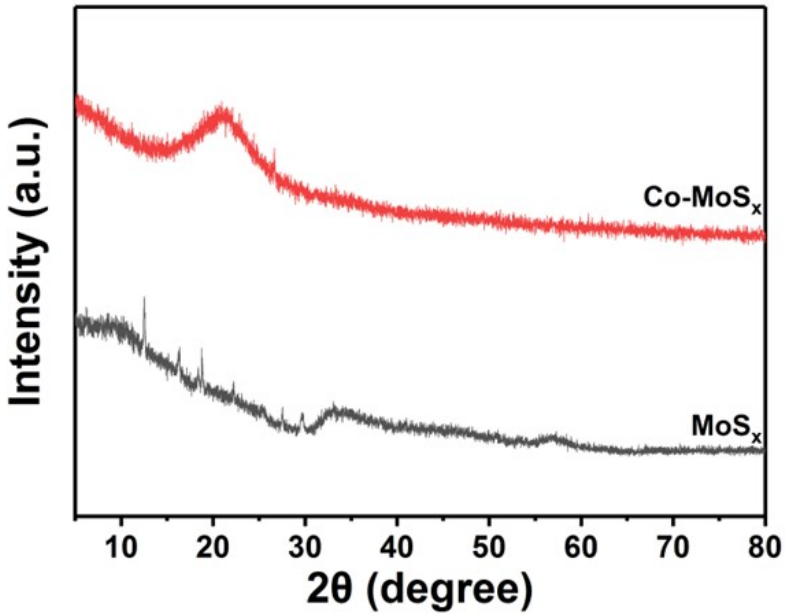

Fig. S2. The XRD patterns of pristine MoS_x and Co-MoS_x.

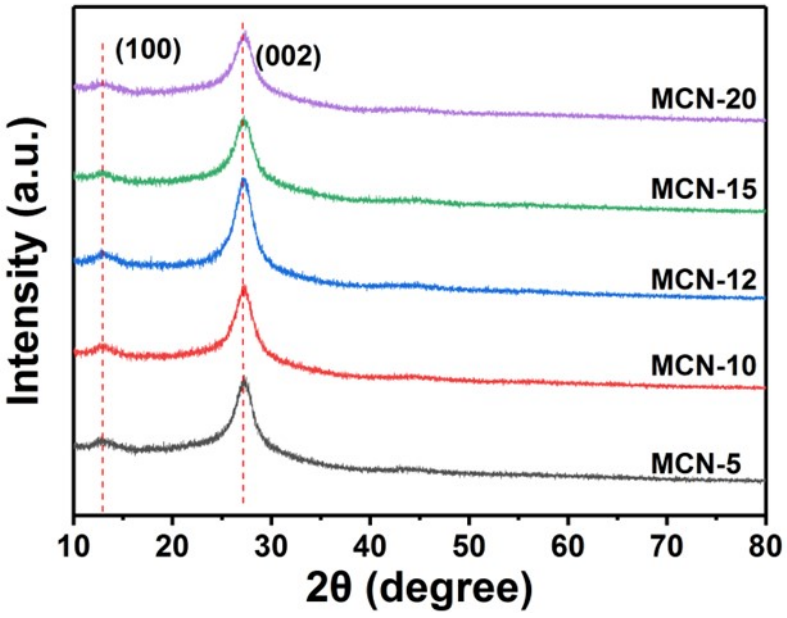

Fig. S3. The XRD pattern of CN with different MoS_x loadings.

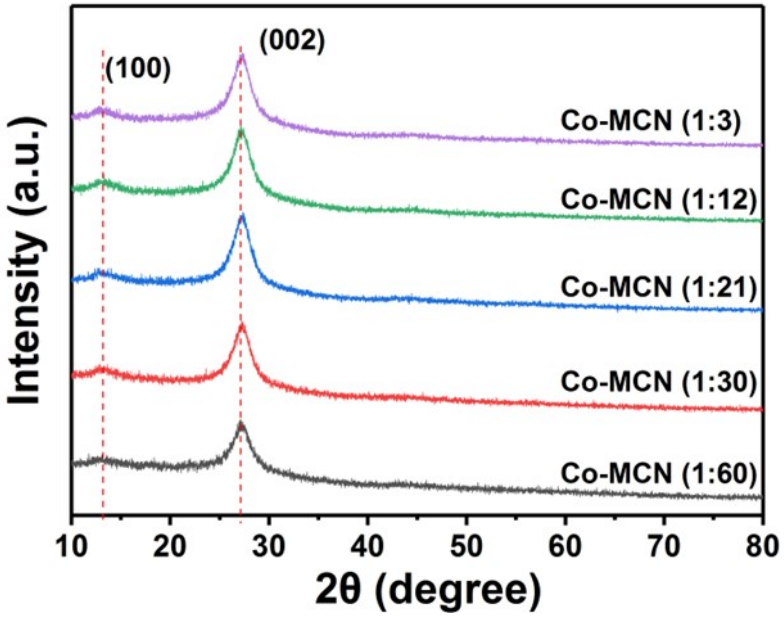

Fig. S4. The XRD pattern of CN with different mass ratios of Co-MoS_x loadings.

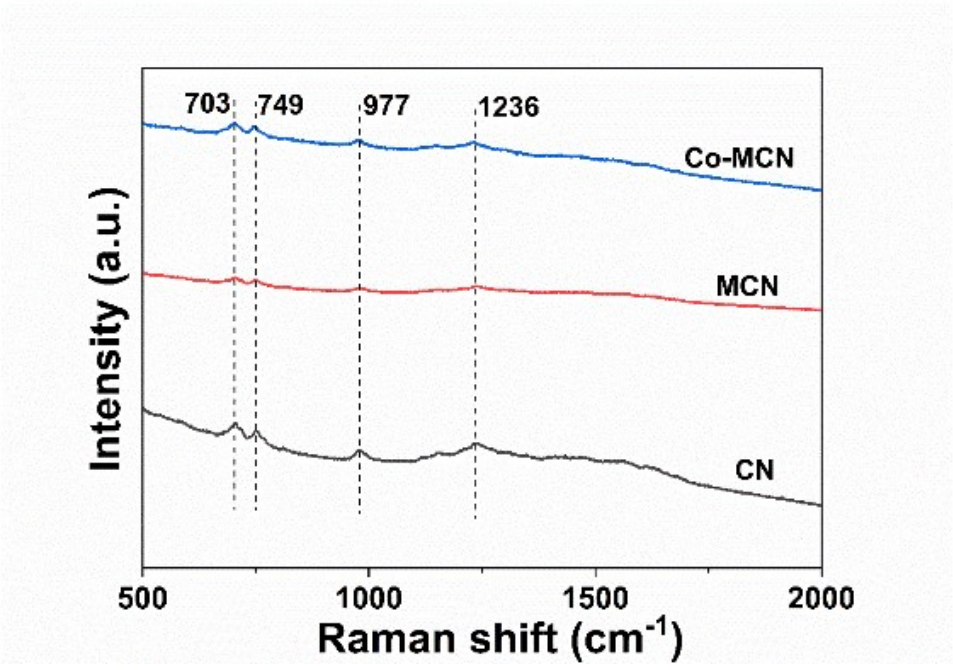

Fig. S5. Raman spectra of CN, MCN and Co-MCN composite photocatalyst.

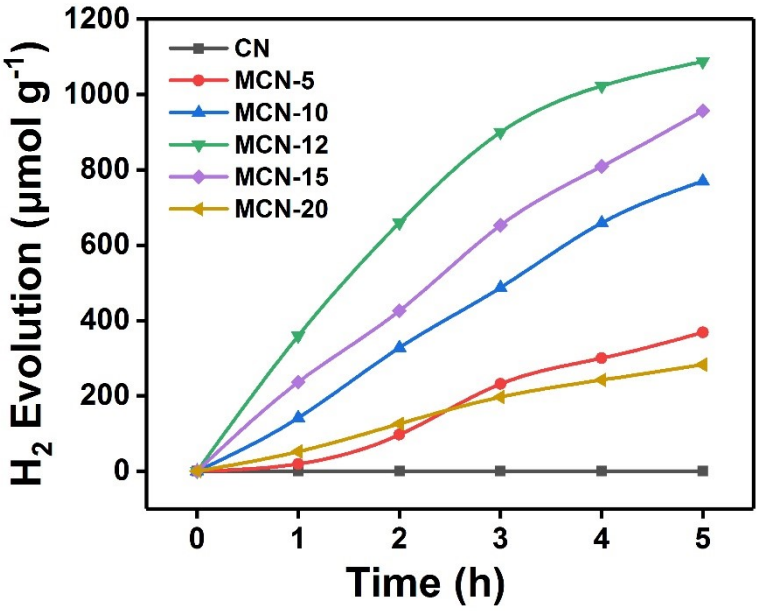

Fig. S6. Hydrogen production capacity of CN with different MoS_x loadings

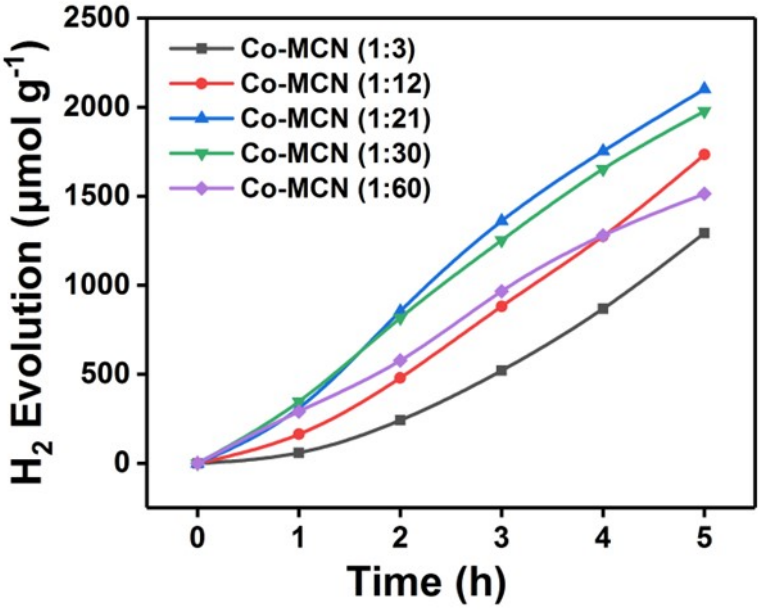

Fig. S7. Hydrogen production capacity of CN with different Co-MoS_x loadings

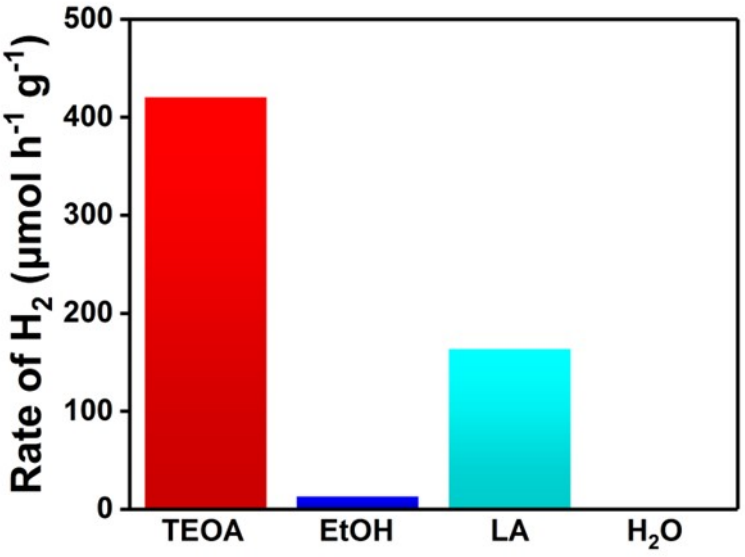

Fig. S8. Hydrogen production rate of Co-MoS_x in different sacrificial reagents

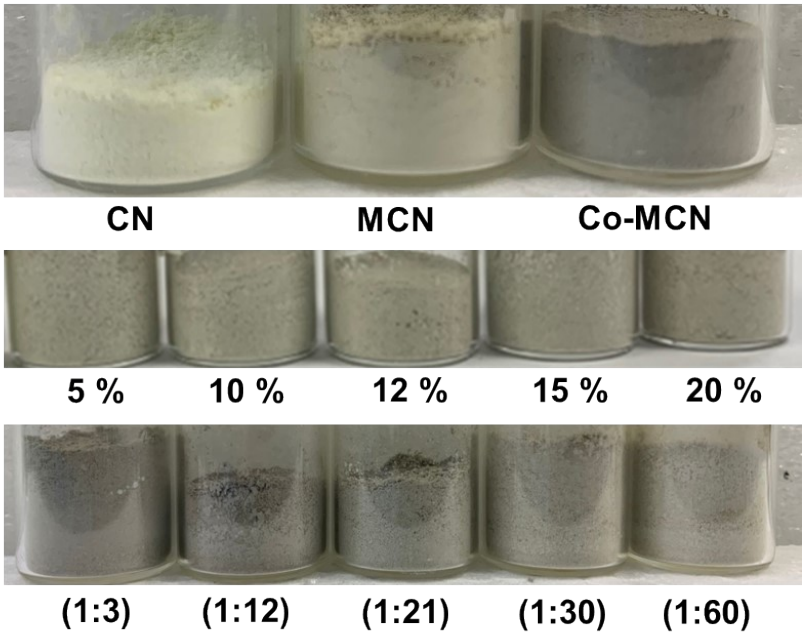

Fig. S9. Digital images of pure CN, MCN and Co-MCN in the first row; The second row shows the digital image of CN with different MoS_x loadings; The third row shows the digital image for different Co-MoS_x loadings of CN.

Table S2. Comparison of the hydrogen production performance of MoS_x/CN and Co-MoS_x/CN obtained in this study with other photocatalytic systems in literatures.

Catalyst	Wavelength (nm)	Sacrificial reagent	H_2 evolution ($\mu mol \cdot g^{-1} \cdot h^{-1}$)	Ref.
MoS_x/CN	λ>400	10 vol% TEOA	217.5	**This work**
Co-MoS_x/CN	λ>400	10 vol% TEOA	420.3	**This work**
MoS_x/CdS	λ>400	10 vol% LA	404.0	2
MoS_x-ND/CN	λ>420	10 vol% LA	164.0	3
MoS_x/CN	λ>400	10 vol% TEOA	1586.0	4
SSCN@MoS_2	λ>420	15 vol% TEOA	91.0	5
MSQD/CN	λ>420	25 vol% MeOH	577.0	6
MoS_2/U-CN	λ>420	10 vol% MeOH	385.0	7
C/MoS_2/CN	λ>400	10 vol% TEOA	238.0	8
NCDS/MoS_2/CN	λ >420	10 vol% TEOA	212.4	9
Ni-Co/V-CNNT	λ>420	10 vol% TEOA	104.7	10
CN/N-d-C/Co NPs	λ>420	20 vol% TEOA	270.0	11

Reference

1 X. Liu, Y. Xue, Y. Lei, F. Wang and S. Min, *ACS Appl. Nano Mater.*, 2018, **1**, 6493–6501.

2 X. Fu, L. Zhang, L. Liu, H. Li, S. Meng, X. Ye and S. Chen, *J. Mater. Chem. A*, 2017, **5**, 15287–15293.

3 X. Wu, W. Zhong, H. Ma, X. Hong, J. Fan and H. Yu, *J. Colloid Interface Sci.*, 2021, **586**, 719–729.

4 X. Li, B. Wang, X. Shu, D. Wang, G. Xu, X. Zhang, J. Lv and Y. Wu, *RSC Adv.*, 2019, **9**, 15900–15909.

5 Q. Gu, H. Sun, Z. Xie, Z. Gao and C. Xue, *Appl. Surf. Sci.*, 2017, **396**, 1808–1815.

6 Y. Liu, H. Zhang, J. Ke, J. Zhang, W. Tian, X. Xu, X. Duan, H. Sun, M. O Tade and S. Wang, *Appl. Catal. B Environ.*, 2018, **228**, 64–74.

7 W. Li, L. Wang, Q. Zhang, Z. Chen, X. Deng, C. Feng, L. Xu and M. Sun, *J. Alloys Compd.*, 2019, **808**, 151681.

8 H. Liang, J. Bai, T. Xu and C. Li, *Adv. Powder Technol.*, 2021, **32**, 4805–4813.

9 Y. Jiao, Q. Huang, J. Wang, Z. He and Z. Li, *Appl. Catal. B Environ.*, 2019, **247**, 124–132.

10 Y. Zhu, X. Zhong, X. Jia and J. Yao, *Environ. Res.*, 2022, **203**, 111844.

11 W. Kong, M. Hong, W.-S. Zou, Q. Li, Y. Xu, Y. Xu, P. Wu, J.

Zhang and Y. Wang, *Int. J. Hydrogen Energy*, 2022, **47**, 38583–38593.